Pure Appl. Chem., Vol. 78, No. 9, pp. 1691–1702, 2006.
doi:10.1351/pac200678091691

Use of metal complexes to synthesize semiconductor nanoparticles*

N. Revaprasadu‡ and S. N. Mlondo

Department of Chemistry, University of Zululand, Private bag X1001, KwaDlangezwa, 3886, South Africa

Abstract: Research in materials with dimensions of the order of nanometers has made a huge impact on the scientific community in the past decade. Chemists play an important role in this area of research as they endeavor to prepare pure, crystalline, surface-derivatized nanoparticles, which can be processed in potential applications. This review describes some of the routes to nanoparticles with particular emphasis on the use of metal complexes in the preparation of high-quality nanoparticles. The synthesis of II/VI semiconductor nanoparticles such as CdSe, CdS, ZnS, and PbS using the single molecular precursor route is reviewed in detail. The synthesis of some III/V semiconductor materials is also briefly discussed. Finally, current work on the shape control of nanoparticles is described. The mechanism of growth induced by variation of reaction conditions is discussed using CdSe nanoparticles as an example.

Keywords: semiconductor nanoparticles; II/VI semiconductors; CdS; cadmium sulfide; nanotechnology; particle shapes.

INTRODUCTION

Research into materials of the order of nanometers has grown exponentially in the past decade. The understanding of the fundamental properties and potential use in technological applications has stimulated the interest in nanomaterials. Much of the earlier work focused on discovering new synthetic routes to nanoparticles, with extensive studies on the chemical and physical properties of the particles also reported [1–4]. Recently, there has been a shift toward the self-assembly of these nanoparticles by either bottom-up or top-down techniques [5–8]. In relation to these studies, there has been a drive to synthesize nanoparticles of various shapes. The morphology of the particles either spherical-, rod-, tetrapod-, or hexagonal-shaped will have an effect on its properties and also influence the self-assembly process [9–15]. This paper will describe some of the recent advances in using chemical routes to synthesize nanoparticles of controllable size and shape. The focus will be on the use of metal complexes as single-molecule precursors to synthesize surface-passivated semiconductor nanoparticles. The shape control of the nanoparticles through variation of experimental conditions will also be highlighted.

Nanoparticles of semiconducting materials with all three dimensions in the range of 1–20 nm have unique properties. These novel electronic, magnetic, catalytical, and optical properties are due to their large surface-to-volume ratio and their reduced size. As the diameter of the particle approaches the exciton Bohr diameter, the charge carriers become confined in three dimensions with zero degrees of

*Paper based on a presentation at the 3rd IUPAC Workshop on Advanced Materials (WAM III), Stellenbosch, South Africa, 5–9 September 2005. Other presentations are published in this issue, pp. 1619–1801.

‡Corresponding author: E-mail: nrevapra@pan.uzulu.ac.za

freedom [16,17]. As a result of the geometrical constraints, the electron feels the particle boundaries and responds to particle sizes by adjusting its energy. This phenomenon, known as the quantum size effect, causes the continuous band of the solid to split into discrete, quantized levels and the "bandgap" to increase (Fig. 1).

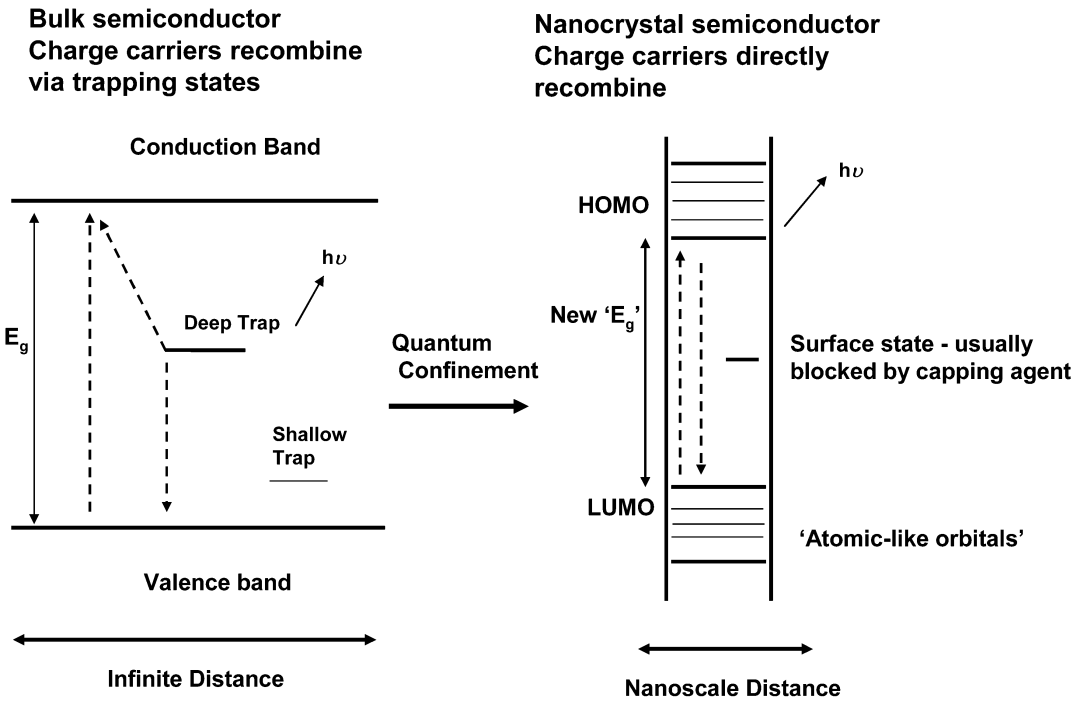

Fig. 1 The spatial electronic-state diagram showing the quantum confinement effect in (a) bulk semiconductors and (b) nanoparticles [19].

The increase in the bandgap is observed by the blue shift in the absorption spectra as seen in many semiconductor nanoparticles. The luminescence spectra of passivated semiconductor nanoparticles have narrow line widths and exhibit a small Stoke's shift or "near band-edge" emission due to the direct recombination of the charge carriers. In contrast, nanoparticles that show broad emission with a larger Stoke's shift are considered to exhibit emission from deep and shallow traps [18].

PREPARATION METHODS

The control of the size, shape, and ease of manipulation of nanoparticles synthesized by chemical routes has rendered this route of synthesis the preferred method of choice in future applications. Traditional chemical vapor deposition and molecular beam epitaxy methods have limitations as they produce particles that are attached to a substrate or embedded in a matrix, thereby limiting their potential in applications. The assembly of nanoparticles into ordered states of matter, forming close-packed solids, opens up the possibility of fabricating devices as the interactions between proximal nanoparticles give rise to new collective phenomena.

COLLOIDAL ROUTES

The colloidal access to nanoparticles is achieved by carrying out a precipitation reaction in a homogenous solution in the presence of stabilizers, whose role is to prevent agglomeration and further growth [18–21]. La Mer et al. [38] explained the synthesis of highly monodispersed colloids by suggesting that if the seeds (nuclei) could be made to grow in concert into larger particles, monodispersed sols could be formed. If the nucleation and growth processes were properly controlled, particles with nanosize dimensions could be reproducibly synthesized. In this process known as Ostwald ripening, small crystals, which are less stable, dissolve and then recrystallize on larger and more stable crystals. For this method to be effective, the nanoparticles must have low solubility, which can be achieved by judicious choice of solvent, pH, and passivating agent. Highly monodispersed samples are obtained if nucleation and growth processes are distinctly separated (i.e., fast nucleation and slow growth). The colloidal growth stability of the crystals can be improved by using solvents with low dielectric constants or by using stabilizers such as styrene/maleic acid copolymer. The reaction between aqueous solution of $CdSO_4$ and $(NH_4)_2S$ is a typical example for the precipitation synthesis of CdS nanoparticles [20]. Spenhel et al. [20,21] and Brus et al. [18] have made significant contributions to this method of preparation especially in the early work on CdS nanoparticles. Although this method of synthesis is efficient, some important semiconductor materials such as CdSe, GaAs, and InP cannot be easily synthesized [19].

PRECURSOR ROUTES

The problems associated with the low-temperature colloidal route could be overcome by injecting precursors that undergo pyrolysis at high temperature into a high boiling point coordinating solvent. This route, pioneered by Bawendi et al. [22,23], uses a volatile metal alkyl(dimethylcadmium) and a chalcogen source tri-*n*-octylphosphine selenide (TOPSe), dispersed in tri-*n*-octylphosphine (TOP) and injected into hot TOPO (tri-*n*-octylphosphine oxide). Nucleation of CdSe nanoparticles was achieved by supersaturation of the concentrated reagents resulting in the formation of nuclei, followed by slower growth and annealing, consistent with an Ostwald ripening process. The particles produced by this method were very monodispersed (±5 %) and crystalline. The synthetic route reported by Bawendi was slightly modified by Alivisatos and coworkers to synthesize InP nanoparticles. $InCl_3$ was reacted with $P(SiMe_3)_3$ in hot TOPO with subsequent annealing of the particles in the presence of a surfactant (dodecylamine). The InP nanoparticles were 2–5 nm in diameter, with the bandgap varying from 1.7 to 2.4 eV [24].

The capping group or surfactant plays an important role in the nanocrystal growth [25]. At high temperatures (200–400 °C), the surfactant molecules are dynamically adsorbed to the surface of the growing crystal, thereby stabilizing the particles in solution and mediating their growth. The surfactants can also be exchanged with other organic molecules with different functional groups and polarity. Examples of high boiling point coordinating solvents used include alkyl phosphates, alkyl phosphites, pyridines, long-chain alkylamines, and furans [25]. Furthermore, the surfactant can be completely removed and an epitaxial layer or shell of another material can be grown onto the initial nanocrystal. There are many examples of these core-shell systems reported in the literature, including CdSe/CdS [26–29], CdSe/ZnS [30–33], CdSe/ZnSe [34], and InP/ZnS [35]. These systems have been reported to have improved luminescence, quantum yields, decreased fluorescence lifetimes, and benefits related to the tailoring of the relative bandgap positions between the two materials.

Single-molecule precursors

The inherent problems associated with the use of toxic and volatile compounds such as metal alkyls at elevated temperatures led to the development of alternative chemical routes to nanoparticles. The use of single-molecule precursors in which the metal-chalcogenide bond is available has proven to be a very efficient route to high-quality nanoparticles. Trindade and O'Brien investigated cadmium dithio- and diselenocarbamate complexes as precursors for the preparation of TOPO-capped II/VI semiconductor nanoparticles [36,37]. This method of preparation involves the dispersion of the precursor in TOP followed by injection into hot TOPO. The formation of the nanoparticles is consistent with the LaMer mechanism for colloids [38]. The decomposition of the precursor drives the formation of the nanoparticles with termination of growth occurring when the precursor supply is depleted. After the initial injection there is rapid nucleation, followed by controlled growth of the nuclei. When the nanoparticles reach a desired size, the further growth is arrested by quickly cooling the solution. The nanocrystals are isolated from the growth solution by adding another solvent that is miscible with the initial solvent, but has an unfavorable interaction with the capping groups, thereby reducing the barriers to aggregation resulting in flocculation. The resultant turbid solution is centrifuged, and the nanoparticles are isolated in the form of a powder. The capped nanoparticles can be dispersed in a variety of solvents for optical or physical measurements.

Initial work by the O'Brien group involved the use of bis(alkyl/selenocarbamato)cadmium(II)/zinc(II) compounds which were thermolyzed in TOPO to give MS and MSe nanoparticles (M = Cd, Zn) [36,37,39–41]. The preparation of these precursors follows a simple procedure in which CSe_2 or CS_2 is reacted with an excess of the amine and hydroxides at temperatures below 0 °C to give the dithio- and diselenocarbamates as the salt. This compound is then reacted with a stoichiometric quantity of aqueous solution cadmium(II)/zinc(II) chloride to give the bis(dialkyl/dithio/diselenocarbamato)cadmium(II)/zinc(II) compounds of the type $M(E_2CNRR')_2$ either containing symmetric amine alkyl groups (R = R' = alkyl) or having asymmetric groups on the amine (R = Me or Et and R' = ^{n}Hex, ^{n}Bu), see reaction Scheme 1.

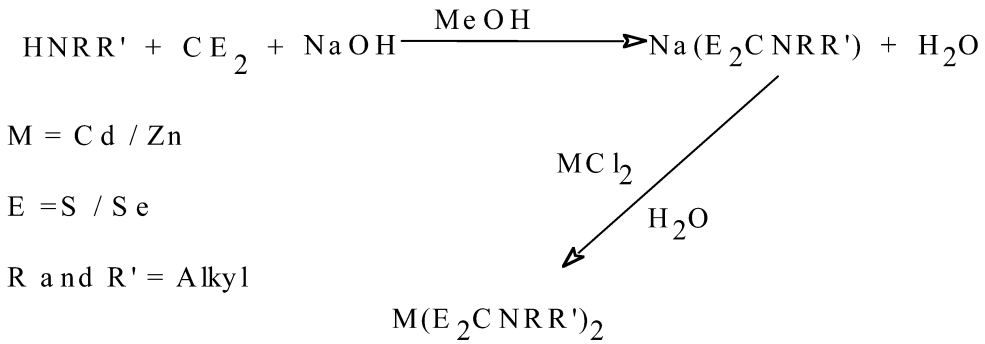

Scheme 1 Schematic reaction for the preparation of single-source precursors.

Subtle changes in substituents at the nitrogen of a diseleno- or dithiocarbamate can markedly affect the thermal decomposition of metal complexes used in the preparation of chalcogenides. Gas chromatography/mass spectrometry (GC/MS) studies have suggested that the decomposition mechanisms of symmetrical diselenocarbamates produce selenium clusters, however, the unsymmetrical diselenocarbamates produce only the metal selenide and organic byproducts [42]. The use of the unsymmetrical, air-stable $[Cd(S_2CNMeHex)_2]$ and $[Cd(Se_2CNMeHex)_2]$ produced monodispersed TOPO-capped CdS and CdSe nanoparticles, respectively (Fig. 2) [39,40]. The optical spectra of the CdS and CdSe showed well-defined excitonic features, and their corresponding photoluminescence spectra were

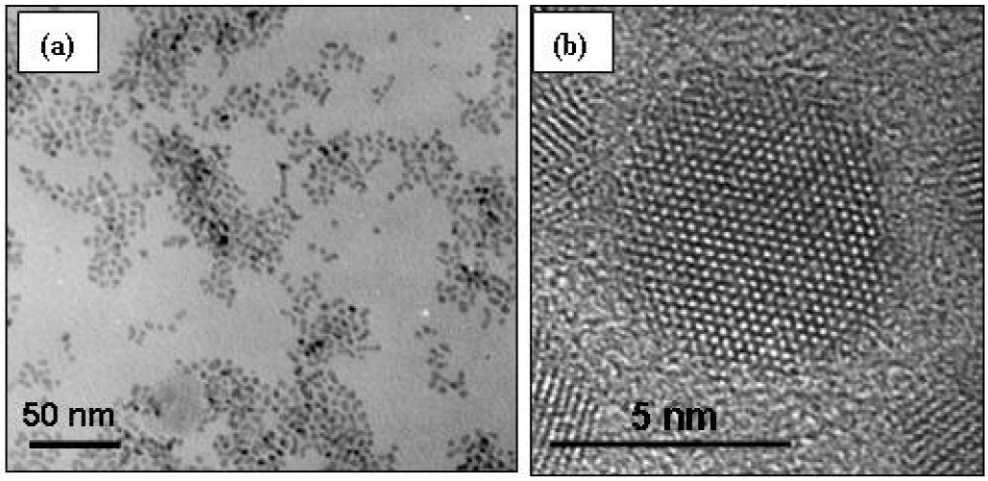

Fig. 2 CdSe nanoparticles synthesized from [$Cd(Se_2CNMeHex)_2$], (a) TEM image showing well-defined articles and (b) high-resolution TEM showing a single nanoparticle (ca. diameter = 5 nm).

Stoke's-shifted in relation to their band edges. A time growth study on CdSe nanoparticles shows that particle growth is linear with time (10 min to 24 h). However, there is a decrease in the standard deviation from ±12.93 to ±8.69 % from the (t = 10 min) to the (t = 30 min) sample, indicating a narrow size distribution. The particle size distribution then increases over 24 h ($\sigma = \pm 10.13$). This trend has been reported previously for CdSe nanoparticles by Alivisatos et al. who explained the phenomena on the basis of classical colloidal chemistry [43]. The initial decrease in size distribution occurs when the CdSe nanoparticles are larger than the critical size at equilibrium, resulting in the faster growth of the smaller particles in relation to the larger particles. The size distribution broadens again when the precursor supply is depleted. This happens because the critical size becomes larger than the average size, resulting in the collapse of the smaller nanoparticles while the larger particles continue to grow.

There have been many other types of precursors all having the metal sulfur bond that have been used for the synthesis of CdS nanoparticles. The closeness in structure of xanthates in relation to dithiocarbamates makes them ideal precursors for CdS nanoparticles. Cadmium ethylxanthate was thermolyzed in TOPO at 160 °C to give monodispersed, spherical TOPO-capped CdS nanoparticles with an average particle size of 4.2 nm [44]. The thermolysis of the identical xanthate precursor in hexadecylamine (HDA) at various temperatures gives rod-shaped CdS nanoparticles [45]. Spherical and nonspherical MS particles (M = Cd, Zn, Pb, Hg, Ni, Cu, Mn) have also been synthesized using metal alkylxanthates in HDA [45]. The authors described the use of reaction time, temperature, and/or concentration to achieve size and spectroscopic tunability of the particles. A cadmium(II) complex of dithiobiurea, $Cd(SCNHNH_2)_2Cl_2$ has also been used to synthesize CdS nanoparticles with a narrow size distribution [46]. A comparative study of CdS nanoparticles synthesized under similar conditions in TOPO using bis(methylhexyldithiocarbamato)-cadmium (II), cadmium ethylxanthate, and a cadmium complex of dithiobiurea, revealed very few differences in the optical and structural properties of the nanoparticles (Fig. 3) [47]. The narrow PL spectra is characteristic of emission from particles of CdS in the 3–5 nm size regime [48,49]. The absorption spectra show excitonic features typical of particles in the nanosize regime. The powder X-ray patterns confirm the wurtzite phase in all samples of CdS.

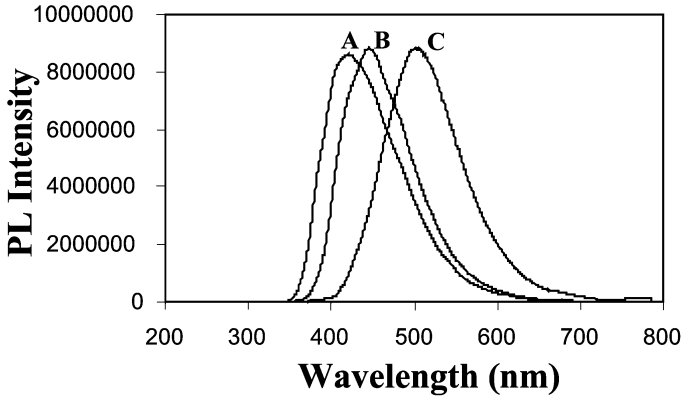

Fig. 3 Photoluminescence spectra of CdS nanoparticles synthesized from: (A) $Cd(NH_2CSNHNH_2)Cl_2$, (B) $Cd(C_2H_5OCS)_2$, and (C) $Cd(S_2CNMeHex)_2$.

Metal complexes of alkylthioureas have also proven to be very good precursors for nanoparticle synthesis. A series of cadmium(II) complexes with *N*-alkyl/aryl and *N*,*N*'-dialkyl/aryl thioureas (RNHCSNHR'; where R = R' = CH_3, CH_2CH_3, C_6H_5, and/or R' = H) were synthesized by Moloto et al. [50]. The $[CdCl_2(CS(NH_2)NHCH_3)_2]$, $[CdCl_2(CS(NH_2)NHCH_2CH_3)_2]$, and $[CdCl_2(CS(NH_2)_2]$ complexes were thermolyzed in TOPO at 200 °C to give CdS with crystallite sizes of 4.8, 4.3, and 32.2 nm from the respective complexes (Fig. 4) [51]. There was evidence of agglomeration in all samples from the transmission electron microscopy (TEM) measurements. Mono- and di-substituted alkylthiourea complexes of lead and copper have been used to prepare PbS and Cu_xS_y nanoparticles [52]. The X-ray diffraction (XRD) pattern of the PbS confirms a cubic rock-salt phase, with the particles having a predominantly truncated octahedral shape. The copper alkylthiourea complex was added directly into the hot TOPO to give a mixture of nanoparticles suspended in solution and bulk material, which settle at the bottom of the reaction flask. The XRD pattern of the nanoparticles gave a mixture of sulfides of two major stoichiometries, $Cu_{1.8}S$ (digenite) and $Cu_{31}S_{16}$ (djurleite). The TEM images showed well-defined, triangular, and hexagonal-shaped particles.

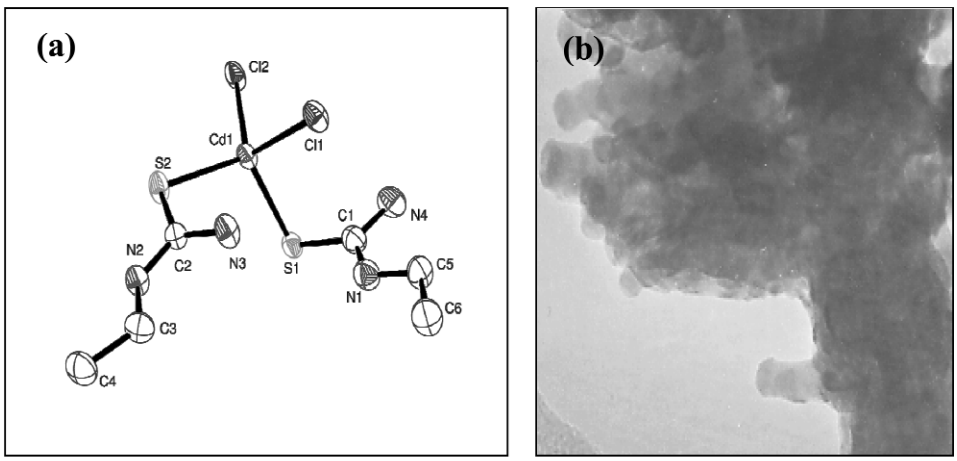

Fig. 4 (a) Single X-ray structure of *N*-ethyl cadmium thiourea and (b) TEM image of CdS nanoparticles synthesized from the cadmium complex [43,44].

PbS and PbSe have also been achieved using various lead dithio- and diselenocarbamates [37]. The inherent cubic shape of the PbS is visible in the TEM images. There has been extensive work reported by Revaprasadu and O'Brien on ZnS [53], ZnSe [41], CuSe [54], InSe [55], InS [55], GaS [56], and PdS [57] nanoparticles synthesized in various coordinating solvents using the respective metal dithio- and diselenocarbamates (Fig. 5).

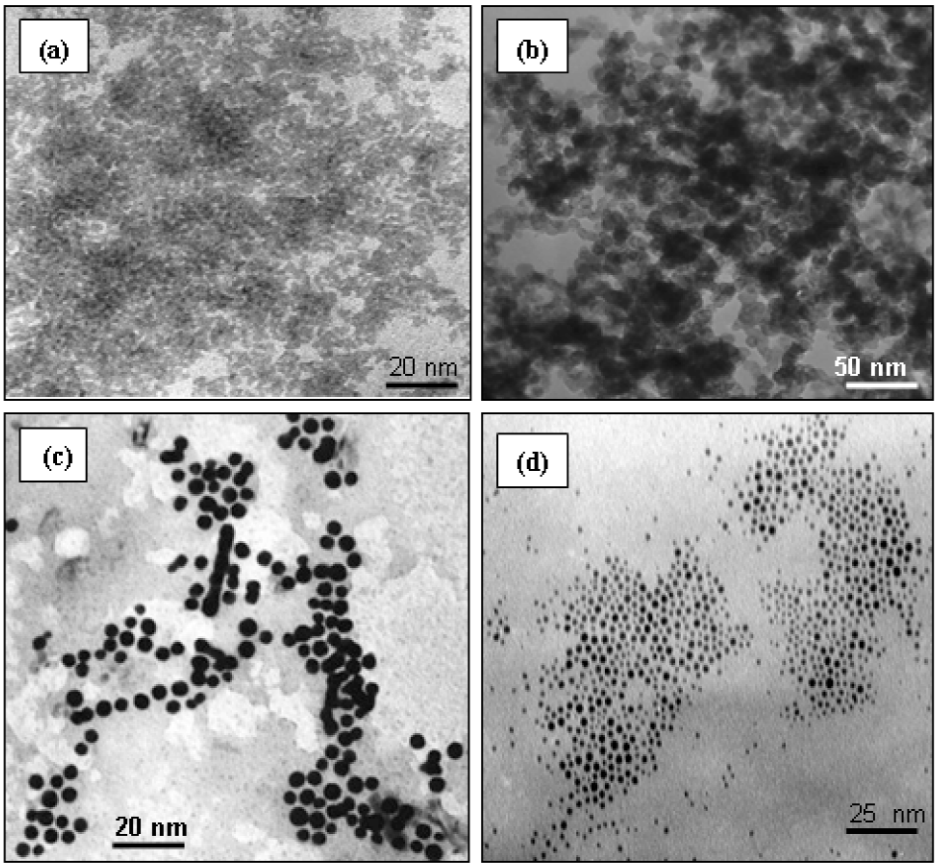

Fig. 5 TEM images of (a) ZnS [53]; (b) CuSe [54]; (c) InSe [55]; and PdS [57] nanoparticles synthesized from the respective dithio/diselenocarbamato metal complexes.

III/V Semiconductors

The preparation of III/V materials is more difficult than their II/VI counterparts due to their increased covalent nature, making separation of nucleation and growth steps difficult [58]. Precursors for III/V materials such as $InCl_3$ coordinate to the reaction solvent inhibiting direct reaction between the reagents. High-quality InP and InAs semiconductor nanoparticles have been synthesized by rapid mixing and heating of III and V precursors in high boiling point coordinating solvents [59]. Typically, $InCl_3$ is used as an In source and reacted with $E(SiMe_3)_3$ (E = As, P) in TOPO to form InP and InAs. Growth and annealing take up to 7 days at ca. 265 °C. Green et al. [60] reported the use of single-molecule precursors such as metal diorganophosphides to synthesize InP and GaP. The compounds $M(PBu^t_2)_3$, (M = Ga, In) were dissolved in 4-ethylpyridine and heated at reflux for up to 7 days. The particles (average diameter = 8 nm) were then isolated by solvent/nonsolvent interactions. The authors also report the use of the same class of precursors for the synthesis of TOPO- and 4-ethylpyridine-capped Cd_3P_2

[61,62]. The particles are stable against photodegradation unlike those prepared by the colloidal route which are air-sensitive and decompose upon illumination. Frank et al. [63] reported the preparation of hexagonal GaN nanoparticles by deprotonation of gallium azides. There have been other routes to the preparation of surface-passivated GaN nanoparticles using cyclotrigallazanes [64] and polymeric precursors [65].

Shape control of nanoparticles

One of the recent trends in nanomaterials research is the control of particle shape. The shape of semiconductor nanocrystals does have significant effect on their electronic, magnetic, catalytic, and electrical properties [66–69]. Metal chalcogenides such as CdSe, CdS, and PbS remain materials of considerable interest in shape control due to their wide variation in 1D morphology with changes in reaction conditions during synthesis.

For a given solution in the synthesis of nanocrystals, one could obtain a variety of shapes (e.g., dots, rods, spindles, and tetrapods). As the size of the nanoparticles decreases to their Bohr radius, all the electronic properties begin to change. In this size regime, the properties become dependent not only on size but also on their shape. For example, if an electron-hole pair (exciton) is formed in a sphere with zero degrees of freedom, the system is known as a "quantum dot". In this system, the exciton is confined in all three dimensions (x,y,z). If the particle is elongated, for example, along the c-axis, the exciton formed will still be confined in the x and y direction (a and b) but can be transported along the z, exhibiting the rod-like structure. This suggests it is confined in two directions but can move along the z-axis. If, on the other hand, the original sphere (dot) is compressed along the z-axis and equally extended in x and y (e.g., nanodisks), the exciton's motion is confined in one direction but has room to move along x and y. These are referred to as 2D structures.

Critical parameters for shape control

The final morphology of nanocrystals in any solution system is governed by the preferred growth regime of the reaction. The reaction can proceed either in a kinetic or thermodynamic growth regime [10,13]. Several critical parameters such as monomer concentration, reaction temperature, and capping group influence the type of growth regime. The thermodynamic growth regime is driven by sufficient supply of thermal energy (high reaction temperature) and low monomer concentration, yielding stable, isotropic-shaped nanocrystals (e.g., dots, cubes). In contrast, nonequilibrium kinetic conditions are facilitated by low reaction temperatures and high monomer concentration yielding selective anisotropic structures (e.g., rods, tetrapods) [10–13].

The surface properties of the nanoparticles can be tailored by the type and amount of adsorbing organic capping molecule. Alivisatos et al. [10] showed that by changing the surface energies through adjustment of the types and ratios of organic surfactants, the shape of CdSe nanoparticles could be controlled. The conditions of the growth of CdSe nanoparticles using a mixture of surfactants can be set such that cubic (zinc blende) nuclei can be formed. However, after the nucleation stage, the conditions could be manipulated to favor the cubic phase, resulting in the formation of large spherical or tetrahedral nanocrystals. To achieve hexagonal (wurtzite) growth, the system has to be kept in the high-temperature kinetic regime or the concentration of the monomers has to be increased.

Thermodynamically, all nanocrystals will grow toward a shape that has the lowest energy at equilibrium. However, the reaction parameters can influence the formation dynamics, thereby allowing for various shapes of particles (Fig. 6) [12]. At low monomer concentrations or lengthy time growth, all nanocrystals grow toward the lowest chemical environment, and this leads to the formation of only dots. A moderate monomer concentration can only support those existing seeds in the 3D growth stage, resulting in the formation of rice- or spindle-shaped particles. At high monomer concentration, the "magic-sized" (extremely small seeds with high potential) nanoclusters promote the formation of rods

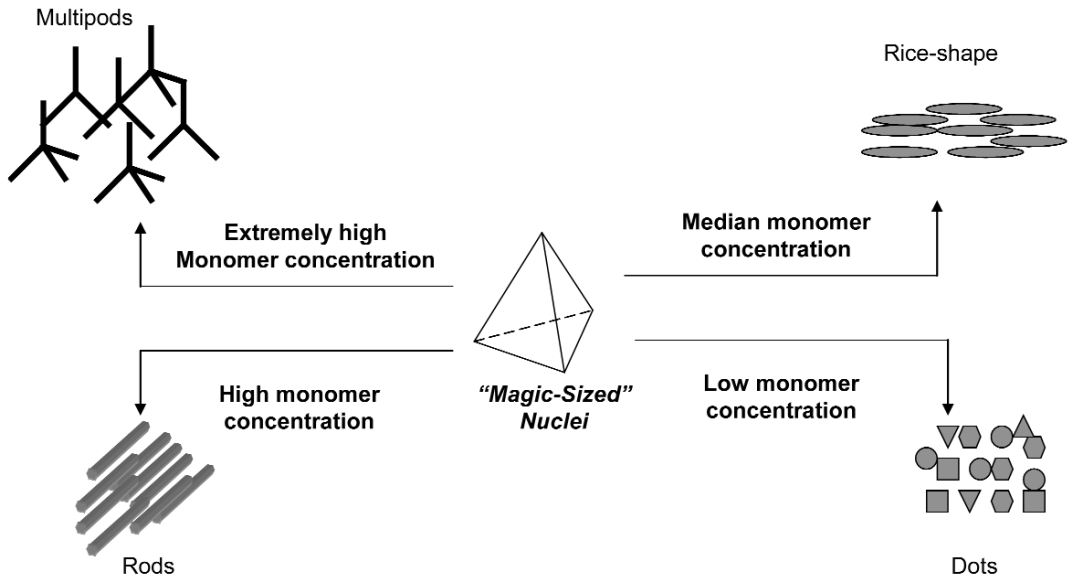

Fig. 6 Monomer concentration-dependent growth patterns of nanocrystals [12].

or other elongated structures. Tetrapod-shaped particles of CdSe and CdS have been reported [10–13]. Extremely high monomer concentrations favor the formation of particles with this shape. The wurtzite-like rods (or arms) form out of the (111) face of the original zinc-blende nucleus.

Colvin et al. [70] reported the observance of tetrapod and rod-like morphologies of CdSe and CdTe. The influence of temperature, monomer concentration, reaction time, and capping group on the particle morphology was also studied by Li et al. [45]. It was found that the thermolysis of cadmium ethylxanthate in hot HDA gave rod- or spherical-shape particles depending on the reaction conditions. Moderate temperatures (<200 °C), high monomer concentration, and long reaction times (3 h) produced long multi-armed nanorods. An increase in temperature (260 °C) induced the formation of short single-armed rods. Recently, the thermolysis of a *N*-alkyldithiocarbamato complex of cadmium, was thermolyzed in HDA to give 1D CdS nanostructures (single, bent, or multi-rods) at moderate to high temperatures [71]. The shape of the nanocrystals varied from longer rods to shorter rods with increased width by simply increasing the quantity of precursor in the bulk solution from 0.05 g/8 ml HDA to 1 g/8 ml HDA at 250 °C.

The shape evolution from spheres to rods is evident with increase in reaction temperature. In a detailed study using cadmium complexes of thiourea complexes, *N*,*N*'-dioctyl thiourea, *N*,*N*'-dicyclohexyl thiourea, and *N*,*N*'-diisopropyl thiourea for the preparation of CdS nanoparticles in a "one-pot" synthesis in TOPO, it was found that at higher temperatures there seems to be the formation of more well-defined rod-shaped particles than those obtained at lower temperatures [72]. The length of the alkyl group also has an effect on the particle morphology. The thermolysis of a thiosemicarbazide complex of cadmium in HDA also gave nanorods of CdS with a bore radius of 6 nm (Fig. 7) [73].

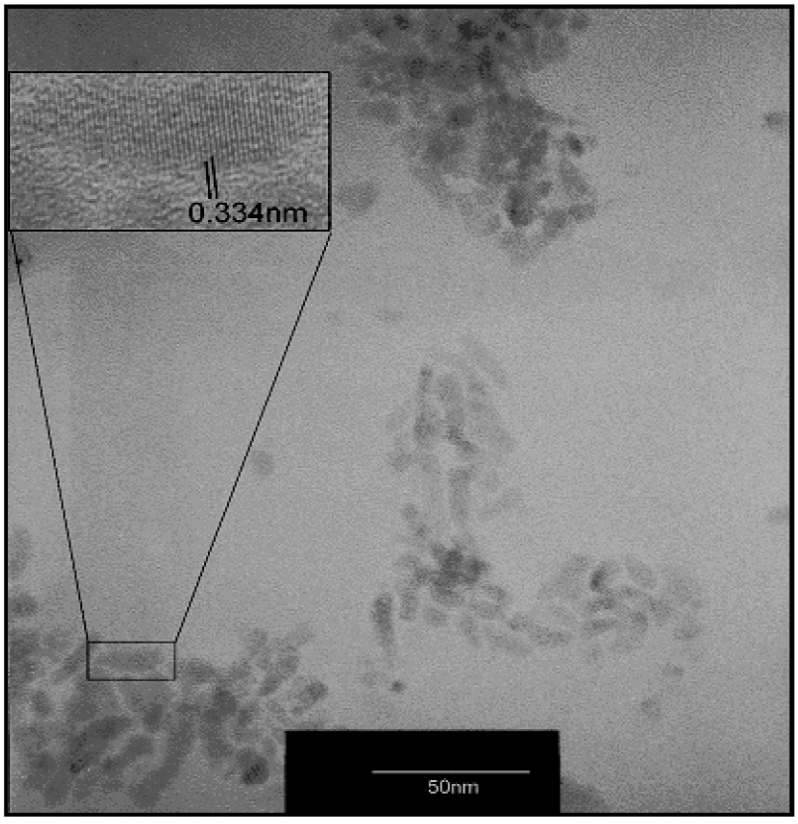

Fig. 7 TEM image of CdS nanorods synthesized from a thiosemicarbazide complex of cadmium in HAD [61].

CONCLUSIONS

The use of metal complexes as single-molecule precursors to synthesize nanoparticles has been identified as a relatively simple and efficient route to high-quality, crystalline, surface-passivated nanoparticles. This "one-pot" synthetic route allows for the control of size and shape through the variation of reaction conditions. Various complexes such as metal complexes of dithio/diselenocarbamates, xanthates, thioureas, and thiosemicarbazides have been successfully used as single-source precursors for the synthesis of II/VI semiconductor nanoparticles. Much work is still ongoing in finding novel complexes that can produce new materials with variable sizes and shapes.

REFERENCES

1. C. B. Murray, K. R. Kagan, M. G. Bawendi. *Ann. Rev. Mater. Sci.* **30**, 545 (2000).
2. M. G. Bawendi, M. L. Steigerwald, L. E. Brus. *Ann. Rev. Phys. Chem.* **41**, 477 (1990).
3. T. Trindade, P. O'Brien, N. Pickett. *Chem. Mater.* **13**, 3843 (2001).
4. A. Henglein. *Chem. Rev.* **89**, 1861 (1989).
5. C. M. Niemeyer. *Angew. Chem., Int. Ed.* **41**, 4128 (2001).
6. M. Sastry. *Pure Appl. Chem.* **74**, 1621 (2002).
7. S. H. Park, H. Yan, J. H. Reif, T. H. LaBean, G. Finkelstein. *Nanotechnology* **15**, S525 (2004).
8. A. Turberfield. *Phys. World* **16**, 43 (2003).
9. L. Manna, E. C. Scher, L. Li, A. P. Alivisatos. *J. Am. Chem. Soc*. **124**, 7136 (2002).

10. X. G. Peng, L. Manna, W. D. Yang, J. Wickham, E. Scher, A. Kandavich, A. P. Alivisatos. *Nature* **404**, 59 (2000).
11. J. Hu, L. S. Li, L. W. Wang, L. Manna, A. Alivisatos. *Science* **292**, 2060 (2001).
12. X. Peng. *Adv. Mater.* **15**, 459 (2003).
13. Z. A. Peng, X. G. Peng. *J. Am. Chem. Soc.* **124**, 3343 (2002).
14. S. M. Lee, Y. W. Jun, S. N. Cho, J. Cheon. *J. Am. Chem. Soc.* **124**, 11244 (2002).
15. Y. W. Jun, Y. Y. Jung, J. Cheon. *J. Am. Chem. Soc.* **124**, 615 (2002).
16. L. Z. Zhang, W. Sun, P. Cheng. *Molecules* **8**, 211 (2003).
17. C. F. Landes, S. Link, M. B. Mohamed, B. Nikoobakht, A. El-Sayed. *Pure. Appl. Chem.* **74**, 1675 (2002).
18. L. E. Brus. *J. Chem. Phys.* **90**, 2555 (1986).
19. M. Green, P. O'Brien. *Chem. Commun.* 2235 (1999).
20. L. Spenhel, H. Hasse, H. Weller, A. Henglein. *J. Am. Chem. Soc*. **109**, 5649 (1987).
21. L. Spenhel, H. Weller, A. Henglein. *J. Am. Chem. Soc*. **109**, 6632 (1987).
22. C. B. Murray, K. R. Kagan, M. G. Bawendi. *Ann. Rev. Mater. Sci.* **30**, 545 (2000).
23. C. B. Murray, D. J. Norris, M. G. Bawendi. *J. Am. Chem. Soc.* **115**, 8706 (1993).
24. M. A. Olshavsky, A. N. Goldstein, A. P. Alivisatos. *J. Am. Chem. Soc*. **112**, 9438 (1990).
25. E. C. Scher, L. Manna, A. P. Alivisatos. *Philos. Trans. R. Soc. London, Ser. B* **361**, 241 (2003).
26. D. V. Talapin, R. Koeppe, S. Goetzinger, A. Kornowski, J. M. Lupton, A. L. Rogach, O. Benson, J. Feldmann, H. Weller. *Nano Lett.* **3**, 1677 (2003).
27. I. Mekis, D. V. Talapin, A. Kornowski, M. Haase, H. Weller. *J. Phys. Chem. B* **107**, 7454 (2003).
28. X. Peng, M. C. Schlamp, A. V. Kandavich. A. P. Alivisatos. *J. Am. Chem. Soc.* **119**, 7019 (1997).
29. X. Chen, Y. Lou, C. Burda. *Int. J. Nanotechnol.* **1**, 105 (2004).
30. A. R. Kortan, R. Hull, R. L. Opila, M. G. Bawendi, M. L. Steigerwald, P. J. Carrol, L. E. Brus. *J. Am. Chem Soc.* **2**, 1327 (1990).
31. M. A. Hines, P. Guyout-Sionnest. *J. Phys. Chem.* **100**, 468 (1996).
32. D. O. Dabbousi, J. Redriguez-Viejo, F. V. Mikulec, J. R. Heine, H. Mattoussi, R. Ober, K. F. Jensen, M. G. Bawendi. *J. Phys. Chem. B* **101**, 9463 (1997).
33. D. V. Talapin, A. L. Rogach, A. Kornowski, M. Hasse, H. Weller. *Nano. Lett*. **1**, 207 (2001).
34. M. Danek, K. F. Jensen, K. F. Murray, C. B. Murray, M. G. Bawendi. *Chem. Mater.* **8**, 173 (1996).
35. S. Haubold, M. Hasse, A. Kornowski, H. Weller. *Chem*. *Commun*. **2**, 331 (2001).
36. T. Trindade, P. O'Brien. *Adv. Mater.* **8**, 161 (1996).
37. T. Trindade, P. O'Brien. *Chem. Mater.* **9**, 523 (1997).
38. T. Jonson, V. K. La Mer. *J. Am. Chem. Soc*. **69**, 1184 (1947).
39. M. A. Malik, N. Revaprasadu. P. O'Brien. *Chem. Mater.* **13**, 913 (2001).
40. B. Ludolph, M. A. Malik, P. O'Brien, N. Revaprasadu. *J. Chem. Soc., Chem. Commun*. 1849 (1998).
41. N. Revaprasadu, M. A. Malik, P. O'Brien, M. M. Zulu, G. Wekefield. *J. Mater. Chem.* **8**, 1885 (1998).
42. M. Chunggaze, M. A. Malik, P. O'Brien. *J. Mater. Chem*. **9**, 2433 (1999).
43. U. Banin, M. Bruchez, A. P. Alivisatos, T. Ha, S. Weiss, D. S. Chemia. *J. Chem. Phys.* **110**, 1195 (1999).
44. P. S. Nair, T. Radhakrishnan, N. Revaprasadu, G. A. Kolawole, P. O'Brien. *J. Mater. Chem.* **12**, 1 (2002).
45. Y. Li, X. Li, C. Yang, Y. Li. *Chem. Mater.* **13**, 2461 (2003).
46. P. S. Nair, T. Radhakrishnan, N. Revaprasadu, G. A. Kolawole, P. O'Brien. *J. Mater. Chem.* **9**, 1555 (2001).
47. P. Sreekumari Nair, T. Radhakrishnan, N. Revaprasadu, P. O'Brien. *Mater. Sci. Technol.* **21**, 237 (2005).
48. S. Gorer, R. M. Penner. *J. Phys. Chem. B* **103**, 5750 (1999).

49. X. Zhang, Y. Xie, Q. Zhao, Y. Tian. *New J. Chem.* **27**, 827 (2003).
50. M. J. Moloto, M. A. Malik, P. O'Brien, M. Motevalli, G. A. Kolawole. *Polyhedron* **22**, 595 (2003).
51. M. J. Moloto, N. Revaprasadu, P. O'Brien, M. A. Malik. *J. Mater. Sci.: Mater. Elect*. **15**, 313 (2004).
52. M. J. Moloto, N. Revaprasadu, G. A. Kolawole, P. O'Brien, M. A. Malik. *S. Afr. J. Sci*. **101**, 463 (2005).
53. N. Revaprasadu, M. A. Malik, P. O'Brien. *J. Mater. Res.* **14**, 3237 (1999).
54. N. Revaprasadu, M. A. Malik, P. O'Brien. *Adv. Mater.* **11**, 1441 (1999).
55. N. Revaprasadu, M. A. Malik, J. Carstens, P. O'Brien. *J. Mater. Chem.* **9**, 2885 (1999).
56. M. A. Malik, P. O'Brien, S. N. Mlondo, N. Revaprasadu. *Mater. Res. Soc. Symp. Proc.* **879E**, Z7.13 (2005).
57. M. A. Malik, P. O'Brien, N. Revaprasadu. *J. Mater. Chem.* **12**, 92 (2002).
58. J. R. Heath, J. J. Shiang. *Chem. Soc. Rev*. **27**, 65 (1998).
59. A. A. Guzelian, U. Banin, A. V. Kadavinach, X. Peng, A. P. Alivisatos. *Appl. Phys. Lett.* **69**, 1432 (1996).
60. M. Green, P. O'Brien. *J. Chem. Soc., Chem. Commun*. 2459 (1998).
61. M. Green, P. O'Brien. *Adv. Mater*. **10**, 527 (1998).
62. M. Green, P. O'Brien. *J. Mater. Chem*. **9**, 243 (1999).
63. A. Frank, F. Stowasser, H. Sussek, H. Pritzkow, C. R. Miskys, O. Ambacher, M. Giersig, R. Fischer. *J. Am. Chem. Soc.* **120**, 3512 (1998).
64. J. F. Janik, R. L. Wells, J. L. Coffer, J. V. St. John, W. T. Pennington, G. L. Schimek. *Chem. Mater.* **10**, 1613 (1998).
65. O. I. Micic, S. P. Ahrenkiel, D. Bertram, A. J. Nozik. *Appl. Phys. Lett.* 75 (1999).
66. C. Burda, X. Chen, R. Narayanan, M. A. El-Sayed. *Chem. Rev*. **105**, 1025 (2005).
67. P. D. Yang, C. M. Lieber. *Science* **273**, 1836 (1996).
68. J. Perez-Juste, I. Pastoria-Santos, L. M. Liz-Marzan, P. Mulvaney. *Coord. Chem. Rev.* **249**, 1870 (2005).
69. J. Hu, L. S. Li, W. Yang, L. Manna, L. W. Wang, A. P. Alivisatos. *Science* **292**, 2060 (2001).
70. S. D. Bunge, K. M. Krueger, T. J. Boyle, M. A. Rogriguez, T. J. Headley, V. Colvin. *J. Mater. Chem.* **13**, 1705 (2003).
71. A. A. Memon, M. A. Malik, M. Afzaal, P. O'Brien. *Mater. Res. Soc. Symp. Proc.* **879E**, Z7.10 (2005).
72. P. S. Nair, M. M. Chili, N. Revaprasadu, P. Christian, P. O'Brien. *S. Afr. J. Sci*. **101**, 466 (2005).
73. S. N. Mlondo, N. Revaprasadu, P. Christian, P. O'Brien. *Mater. Res. Soc. Symp. Proc.* **879E**, Z7.6 (2005).